Comments on "Dehydration of hot oceanic slab at depth 30–50 km: Key to formation of Irankuh-Emarat Pb-Zn MVT belt, Central Iran" by Mohammad Hassan Karimpour and Martiya Sadeghi

Abdorrahman Rajabi[1]*, Pouria Mahmoodi[2], Ebrahim Rastad[2], Shojaeddin Niroomand[1], Carles Canet[3], Pura Alfonso[4], Amir Ali Tabbakh Shabani[5], Ali Yarmohammadi[2]

1-School of Geology, College of Science, University of Tehran, Tehran, Iran

2-Department of Geology, Faculty of Basic Sciences, Tarbiat Modares University, Tehran 14115-175, Iran

3-Centro de Ciencias de la Atmósfera, Universidad Nacional Autónoma de México, Del. Coyoacán, 04150 Ciudad de México, Mexico

4-Dept. d'Enginyeria Minera, Industrial i TIC, Universitat Politècnica de Catalunya, Av. de les Bases de Manresa 61-73 o8242 Manresa, Spain

5-Department of Geochemistry, Faculty of Earth Sciences, Kharazmi University, Iran

*** Corresponding author: rahman.rajabi@ut.ac.ir**

Abstract

The Malayer-Esfahan Metallogenic belt (MEMB), in the southwestern Iran, contains numerous different types of the sediment-hosted Zn-Pb (±Ba±Ag), volcanic-sediment hosted Zn-Pb±Ba, sideritic Fe-Mn-Pb (±Ba±Cu), and barite mineralizations. These deposits are hosted mostly in Jurassic shales and sandstones and in Early to Late Cretaceous carbonates and siltstones with minor volcanic rocks. In contrast to the orogenic-related Mississippi Valley type (MVT) deposits, the MEMB deposits formed in an extensional back-arc environment and are characterized by their stratabound and stratiform orebodies. In these deposits, silicification and dolomitization (± sericitization) are the main wall-rock alteration styles. The presence of primary laminated sulfides, fine-grained disseminated sphalerite and galena in association with framboidal pyrite, sedimentary structures in sulfide laminae and bands, and the association of some tuffaceous and volcanic rocks with sulfide mineralizations, along with replacement ore textures in the MEMB deposits are not compatible with orogenic-related MVT model for these mineralization. These characteristics in the Cretaceous MEMB deposits are more compatible with a sub-marine hydrothermal system with sub-seafloor replacement mineralization (e.g., Irish type). Some deposits also share characteristics between Irish type and volcanogenic massive sulfide (VMS) deposits, called VSHMS in this paper. The main argument against the MVT model of Karimpour and Sadeghi (2018) is that this model is not acceptable for the MEMB deposits and could not explain metallogenic aspects of the Zn-Pb (±Ba±Ag) and other mineralizations in this belt.

Keywords:

Malayer-Esfahan Metallogenic belt (MEMB), Mississippi Valley Type (MVT) deposits, back-arc basin, sediment-hosted Zn-Pb (±Ba±Ag), sub-seafloor replacement

The Malayer-Esfahan Metallogenic belt (MEMB) in southwestern Iran (Figs. 1a and 2) contains an enormous accumulation of different types of the sediment-hosted Zn-Pb (±Ba±Ag), Fe-Mn-Pb (±Ba±Cu) and barite mineralizations (Rajabi et al., 2012; Hou and Zhang, 2015). We appreciate the effort and contribution of Karimpour and Sadeghi (2018) on the origin of the sediment-hosted (SH) Zn-Pb (±Ba±Ag) deposits in Malayer-Esfahan metallogenic belt (MEMB), Sanandaj-Sirjan tectonic zone (SSZ). Karimpour and Sadeghi (2018) proposed a genetic model for these deposits, based on field work and Pb isotope geochemistry on galena in some selected deposits and presented a discussion on the role of dehydration of hot oceanic slab in the formation of MVT deposits. However, we have been working on the MEMB for more than 20 years (especially by third author, Rastad), resulting in twenty-four MSc and PhD theses and dissertations on the mineralization in this belt. Based on our geological field experiences, mineralogical and geochemical data, we wish to comment on the conclusions of Karimpour and Sadeghi (2018) and would like to address the following arguments:

1) Most of the SH Zn-Pb (±Ba±Ag) deposits in the MEMB are formed in an extensional back-arc environment (Rajabi et al., 2012).
2) These deposits are not typical orogenic-related Mississippi valley type (MVT) deposits introduced by Bradley and Leach (2003), but they are compatible with sub-marine hydrothermal system as sub-seafloor replacement (e.g., Irish type or Red Dog?) mineralization, and some of them are transitional between Irish type and volcanogenic massive sulfide (VMS) deposits, we call them VSHMS in this paper.
3) Slab was supposedly 35 to 45 degrees dipping (Fig. 14 in Karimpour and Sadeghi, 2018) and such a steep angle have induced slab roll-back (and far-field rifting and high heat flow). Therefore, the low radiogenic Pb isotopes (Mirnejad et al., 2011; Haghi et al., 2019) in these deposits also can indicate that they had a mantle source and were contaminated by continental rocks in an extensional back-arc environment due to a slab roll-back.

First, Karimpour and Sadeghi (2018) claim that the SH Zn-Pb (±Ba±Ag) mineralizations in the MEMB are linked to the orogenic thrust zones and formed in a forearc tectonic setting without discussing the geology or the tectonic setting of the SSZ, MEMB and these deposits during the Mesozoic. Karimpour and Sadeghi (2018) propose that these deposits occurred in the early stage of Neo-Tethys subduction (Late Cretaceous?, abstract, line 20), whereas many researchers believe that subduction initiated in the Jurassic or even Late Triassic (Stampfli and Borel, 2002; Ghasemi and Talbot, 2006; Bagheri and Stampfli, 2008; Mohajjel and Fergusson, 2014). Recent observations from the ophiolites (Fig. 1a) and igneous rocks show that the suture zone between the SSZ and CIM is, in fact, a complex structure formed by an ocean-crustal floored back-arc basin (Shahabpour, 2005; Bagheri and Stampfli, 2008; Moghadam et al., 2009; Mohajjel and Fergusson, 2014) that is known as the Malayer-Esfahan (or Nain-Baft) super basin. The development of the SSZ is related to the generation of the Neo-Tethys Ocean in the Permian to Triassic and its subsequent destruction due to the convergence and continental collision between the Arabian and Iranian plates during the Eocene to lower Miocene time (Mohajjel et al., 2003; Agard et al., 2005; Ghasemi and Talbot, 2005). Subduction of the Neo-Tethys oceanic crust beneath the southern margin of the Iranian Plate (including the SSZ) occurred in the Late Triassic (Bagheri and Stampfli, 2008; Moghadam et al., 2009). Subduction led to the development of arc magmatism in the SSZ from Late Triassic to the Cretaceous (Azizi and Jahangiri, 2008; Mohajjel and Fergusson, 2014) and obduction of Neo-Tethys ophiolite preserved in the Sarv-Abad, Kermanshah and Neyriz areas (Ghazi et al., 2003; Moghadam et al., 2010; Moghadam and Stern, 2011). The convergence between the Arabian and Iranian plates (Fig. 1b, 1c) also led to the opening of the Malayer-Esfahan and Nain-Baft basins between the SSZ and Central Iranian Microcontinent (CIM) (Fig. 1c) and deposition of related extensive Early Cretaceous sediments (Shahabpour, 2005; Bagheri and Stampfli, 2008; Moghadam et al., 2009). During the Late Cretaceous, the north and north-eastward migration of the SSZ arc, the Nain-Baft oceanic crust began to subduct under the CIM (Ghasemi and Talbot, 2005; Moghadam et al., 2009). The closure of the back-arc basin generated the Late Cretaceous to Palaeocene ophiolitic melanges in the Shahr-e-Babak, Dehshir, Nain and Baft areas (Fig. 2) (Bagheri and Stampfli, 2008). Therefore, if the formation of MVT deposits is related to the "dehydration of hot oceanic slab during the early stages of subduction", as suggested by Karimpour and Sadeghi (2018), we would expect to see these deposits in the Triassic or Jurassic rocks, not within the Early Cretaceous units.

Second, the main assumption of Karimpour and Sadeghi (2018) in their paper is that the SH Zn-Pb (±Ba±Ag) deposits of the MEMB are orogenic-related MVT without providing sufficient geological, mineralogical and textural evidences and discussion. But detailed geological investigation on some of these deposits (e.g., Irankuh and Tiran mining district, Robat, Khanabad, Ahangaran, Eastern Haft-Savaran, Darrehnoghreh, Salehpeyghambar, Kuhkolangeh, Lakan, Shamsabad and Sarchal deposits) indicates that most of these deposits are really different from orogenic-related MVT. Here we would like to mention some points that are not compatible with the model suggested by Karimpour and Sadeghi (2018):

A) The SH Zn-Pb (±Ba±Ag) deposits of the MEMB occur in several different stratigraphic horizons/positions (Figs. 3 and 4). This emphasizes that the host strata (the host basin) is the significant ore controlling factor in the formation of these deposits, not the younger thrust faults. Moreover, many of these mineralizations occur adjacent to syn-sedimentary normal faults and their formation is not related to the thrust belts.

B) Leach et al. (2005, 2010) proposed that MVT deposits form in relation to the development of foreland basins in front of an orogeny in a carbonate platform (Fig. 5a), and have no obvious genetic association with igneous rocks and activities (see Figures 2 and 3 in Leach et al., 2010). But detailed geological studies in the MEMB indicate that many of the SH Zn-Pb (±Ba±Ag) deposits in this belt are associated with minor submarine volcanism (Figs. 3 and 4) within the Early Cretaceous sedimentary sequence (e.g., Tiran Mining District, Yarmohammadi et al., 2016; Irankuh Mining District, Boveiri et al., 2017; Golpaygan Mining District, Fadaei, 2018; Fadaei et al., 2016; Eastern Haft-Savaran deposit, Mahmoodi, 2018). Moreover, some of them are hosted directly by the Early Cretaceous volcanic or volcano-sedimentary rocks (e.g., Darrehnoghreh deposit, Rajabi et al., 2012; Fadaei et al., 2016; Salehpeyghambar deposit, Fadaei, 2018), and some of the Fe-Mn-Pb (±Ba±Cu) deposits (e.g., Ahangaran, Shamsabad and Sarchal, Rajabi, 2015; Akbari, 2017; Peernajmodin, 2018) are hosted within the Early Cretaceous siltstones, sandstones and tuffaceous rocks.

C) Barite is typically minor or absent in MVT deposits (Leach et al., 2005; p. 563), but this mineral is an important gangue mineral in the MEMB, replaced by coarse-grained galena and sphalerite (e.g., Irankuh and Tiran mining districts, Robat and Kuhkolngeh deposits) and some of the barite ores are economic (e.g., Robat II deposit).

D) Dolomitization is the most important alteration in MVT deposits but silicification is rare or absent (Leach et al., 2005; Sangster D.F., pers. comm.). However, silicification is one of the major hydrothermal alterations in the MEMB deposits. Also unlike to what Karimpour and Sadeghi (2018) assumed in their article, silicification is the major hydrothermal alteration at the Emarat (Ehya et al., 2010), Lakan, Robat, Kuhkolangeh (Peernajmodin et al., 2018; Haghi et al., 2019), Khanabad and Eastern Haft-Savaran deposits (Mahmoodi, 2018).

E) MVT deposits are typically Cu-poor (Leach et al., 2005), while in most of the MEMB deposits chalcopyrite and tetrahedrite are abundant (Boveiri et al., 2015; 2017; Yarmohammadi et al., 2016), even more than in SEDEX deposits from the CIM (Rajabi et al., 2015a,b).

F) The ore fluids in MVT deposits are basinal brines with ~10 to 30 wt. % NaCl equiv. and temperatures of ore deposition typically from 75° to about 200°C. Fluid inclusion studies on the MEMB SH Zn-Pb (±Ba±Ag) deposits indicate high temperature ore fluids, in the range of 100° to ~325°C with salinity from 2 to 24 wt. % NaCl equiv. (Yarmohammadi et al., 2016; Boveiri et al., 2017; Boveiri and Rastad, 2018; Haghi et al., 2019), which is not consistent with MVT ore fluids and is more compatible with sub-marine hydrothermal mineralization formed via replacement.

G) Detailed mineralogical and textural studies on the MEMB SH Zn-Pb (±Ba±Ag) deposits generally indicate two (or three in some deposits) main paragenetic types of sulfides that are common in most of these deposits (e.g., Irankuh and Tiran mining districts, Robat, Eastern Haft-savaran, Lakan and Khanabad deposits): (1) deposition of volumetrically minor, early, fine-grained, disseminated (to laminated in some of them, Fig 6d, e) sulfides and euhedral barite in unconsolidated sediments at or near the seafloor (Rajabi et al., 2012; Boveiri et al., 2017; Mahmoodi et al., 2019), which in most deposits are associated with large content of framboidal pyrite (Yarmohammadi et al., 2016; Boveiri et al., 2017; Mahmoodi et al., 2018; Peernajmodin et al., 2018; Rajabi and Mahmoodi, 2018). These sulfides and barite are followed by (2) the main coarse-grained sulfide mineralization and extensive sub-seafloor replacement of barite, carbonates and early sulfide laminae/bands by sulfides, and hydrothermal minerals such as quartz, dolomite and siderite within the host siltstone and/or limestone units. (3) A last generation of sulfide minerals is observed in some deposits (e.g., Irankuh and Tiran mining districts; Yarmohammadi, 2015; Boveiri et al., 2017) and includes coarse-grained sphalerite and galena with minor pyrite concentrated in some reverse fault zones due to the later orogenic movements. In these faults, both sulfide minerals and the host rocks show signs of intense deformation.

The fine-grained nature of sulfides at the beginning of mineralization (type 1) reflects rapid crystallization sub-seafloor in unconsolidated mud, likely caused by mixing of seawater with ascending metalliferous fluids (Herzig and Hannington, 1995; Kelley et al., 2004a,b; Kelley and Jennings, 2004). Textures and mineral assemblages similar to type 1 sulfides have also been described in the CIM SEDEX deposits (Rajabi et al., 2015a,b). Similar textures also have been reported at the Red Dog deposits, Alaska, USA (Kelley et al., 2004a,b; Kelley and Jennings, 2004); however, they have been interpreted as the result of the sulfide deposition mainly at the subsurface by impregnation in unconsolidated organic-rich muds.

H) Except the SH Zn-Pb (±Ba±Ag) deposits, there are several unusual Fe-Mn-Pb (±Ba±Cu) deposits in the northwestern part of the MEMB that are hosted in both siliciclastic and volcanic rocks (e.g., Ahangaran, Sarchal, Fig. 6c; Shamsabad, Ghezeldar and Saki deposits) and that represent transitional characteristics between SEDEX and volcanogenic massive sulfide deposits (Rajabi, 2015; Akbari, 2017; Peernajmodin, 2018). In these deposits Fe-bearing carbonates (siderite and ankerite) are the most important hydrothermal minerals that are associated with barite, chalcopyrite, pyrite and galena (e.g., Ahangaran, Sarchal and Shamsabad deposits). Presence of such abundant Fe carbonates associated with barite and sulfides is not common in MVT deposits, but can form by sub-seafloor replacement mineralizations in an extensional environment, with associated submarine volcanism, and are most common in sideritic Fe-Mn-Pb (±Ba±Cu) ore deposits.

I) Fe-rich dolomite (or ankerite) is one of most frequent carbonate alteration observed in the MEMB deposit (Mahmoodi et al., 2019; Boveiri and Rastad, 2018). This carbonate may have formed as the typical alteration of sub-marine hydrothermal sediment-hosted hydrothermal deposits (Lydon, 1996).

J) MVT deposits are hosted mainly by dolostone, limestone and rarely sandstone (Leach et al., 2005), while most of the MEMB deposits occur in carbonate and siltstones or shales. Moreover, in some cases they are hosted by tuffaceous rocks or associated to submarine volcanic rocks (Fig. 4).

K) Detailed tectonic studies and measurement of kinematic indicators in Tiran and Irankuh mining districts and also in Eastern Haft-Savaran, Shamsabad and Ab-Bagh II deposits suggest that the formation of these deposits are related to syn-sedimentary normal faults of the Early Cretaceous (Yarmohammadi et al., 2016; Boveiri et al., 2016; Mahmoodi, 2018; Peernajmodin, 2018; Movahednia et al., 2018), some of which were subsequently reactivated as reverse faults after the Late Cretaceous tectonic event (Nakini, 2013; Boveiri, 2016; Yarmohammadi, 2015). Yarmohammadi (2015) reported some igneous components, sedimentary breccias and debris flows adjacent to the normal fault at the Vejin-Paein deposit. Debris flows and sedimentary breccias abruptly increase in thickness toward the normal faults. Interfingering of debris flows with fine-grained sediments, along with abrupt lateral changes in facies and thickness, indicate the proximity of a synsedimentary faults (Goodfellow, 2004; Rajabi et al., 2015a).

L) In addition to the Early Cretaceous SH Zn-Pb (±Ba±Ag) and Fe-Mn-Pb (±Ba±Cu) deposits, there are enormous shale-hosted SEDEX-type deposits hosted in the Late Jurassic black shales, siltstones and sandstones, which also are related to back-arc extension (e.g., Hossein-Abad, Gol-e-Zard, Ab-Bagh I, Western Haft-Savaran; Mahmoodi et al., 2018; Movahednia et al., 2018). In addition, many volcanogenic massive sulfide deposits are identified in the Jurassic rocks (e.g., Bavanat, Sargaz and Chahgaz deposits; Mousivand et al., 2011; 2018) and in the Cretaceous rocks (e.g., Barika and Abdolsamadi deposits; Yarmohammadi, 2006; Mousivand et al., 2018) of the SSZ. The presence of these ore deposits in the same basin, along with the Early Cretaceous deposits indicate a complex tectonic and metallogenic history of the SSZ which is not explainable with the model of Karimpour and Sadeghi (2018).

M) Some of the MEMB SH Zn-Pb (±Ba±Ag) deposits occur concordantly within the silicified and dolomitized limestone (Fig. 6a,b), at the contact between the Early

Cretaceous massive orbitolina-bearing limestone and the Upper Shale and marl units (e,g., Emarat, Robat, Kuhkolangeh, Lakan and Muchan), which show tabular shapes (Fig. 6a,b,c; also see figure 3 in Ehya et al., 2010). However, they are stratabound, since their shapes are concordant with the host layers and experienced the same folding systems due to the post ore compressional tectonism. In addition, some mineralizations, such as the Sarchal Fe-Mn-Pb (±Ba±Cu) deposit, are completely tabular and hosted in Early Cretaceous siltstones and tuffaceous rocks (Fig. 6c). This indicates that orebodies formed before the compression and that are not related to the thrust fault systems.

Third, Lead geochemistry:

Another major assumption of Karimpour and Sadeghi (2018) in their paper is based on lead isotope dating of galena by Liu et al. (2015), which suggests an age of 66 Ma for the Irankuh mineralization. Subsequently, based on this dating, they concluded that "the age of Irankuh-Emarat Pb-Zn deposits is related to early stage of Neo-Tethys oceanic subducted slab". As we said before, there are at least three sulfide generations at the most of the MEMB SH Zn-Pb (±Ba±Ag) deposits. Therefore, isotope composition of ore deposits can be extremely complicated to interpret. The first question about the isotope dating by Liu et al. (2015, 2018) is that which generation of galena and pyrite were analyzed. A quick look at the paragenetic sequence of the Irankuh mining district on figure 6 in Karimpour and Sadeghi (2018) and on Liu et al. (2015; 2018) show that they did not separate different sulfide generations in their studies; so, it is impossible to fully evaluate the accuracy of the lead isotope dating of Liu et al. (2015) and model obtained by Karimpour and Sadeghi (2018). Furthermore, it is often difficult to determine the absolute age of galena directly with precision, and several analyses of galena from one deposit can give different ages (Rasskazov et al., 2010a,b; Dickin, 2018). Lead model age of galena can be older or younger than their geological ages, even some have model age in the future (Allegre et al., 2008; Dickin, 2018). Therefore, due to the mobility of Pb during geological processes, the galena method is largely discredited as a dating tool, although it may provide powerful constraints on the Earth's evolution (Tosdal et al., 1999; Allegre et al., 2008).

Other comments:

a) On Table 2, Karimpour and Sadegi (2018) introduced a limited number of Zn-Pb deposits, which are presented as MVT deposits. However, mineralogy, fluid inclusions, host rocks, ore textures and sulfide paragenesis and even geochemistry of these deposits differ from MVT mineralization.

b) Parallelism of the SSZ and Urumieh-Dokhtar (UD) magmatic belt is not a reason that supports genetic relationships between ore deposits in these belts, inasmuch as these zones are different in tectonic environment and metallogenic history. The SSZ experienced Jurassic arc magmatism and the Late Jurassic to Early Cretaceous back arc environments, whereas the UD is denoted by Tertiary arc to post orogenic magmatism.

c) Contrary to what Karimpour and Sadegi (2018) claim, many outcrops of volcanic rocks have been reported from Irankuh mining district (Boveiri et al., 2017), Tiran mining District (Yarmohammadi et al., 2016), Golpaygan Mining District (Fadaei et al., 2016, Fadaei, 2018), Ahangaran (Akbari, 2017) and Sarchal areas.

d) The Early Cretaceous-hosted SH Zn-Pb (±Ba±Ag) deposits occur around the Nain-Baft and Sabzevar suture zones, far from the Zagros thrust zone (ZTZ i.e. the collision suture between the Arabian and Iranian plates; Figs. 1a,b, 2, 5c). If Early Cretaceous-hosted Zn–Pb deposits formed due to the collision of the Arabian and Iranian plates, or dehydration of a Neo-Tethys oceanic subducted slab under the SSZ (in a forearc environment), it is so difficult to explain the presence of numerous Early Cretaceous SH Zn-Pb (+Ba+Ag) and other VHSMS deposits in the MEMB and also the YAMB (Yazd-Anarak metallogenic belt in the CIM), in both sides of the Malayer-Esfahan super-basin (Figs. 2, 5b,c; for a detailed explanation see Rajabi et al., 2012).

e) According to the presence of VSHMS deposits in the MEMB (e.g., Darrehnoghreh and Salehpeyghambar), it is possible that slab fluids resemble VSHMS-forming fluids. Therefore, what triggered mineral precipitation must have been T and pH changes near the seafloor, which differs from a mineralizing process in a forearc setting.

In conclusion, Karimpour and Sadeghi's paper (2018) has abundant omissions in the geological data and their interpretation, besides that suggestions and conclusions are ambiguous and over interpretative. The model they presented is speculative and based on incomplete data. In their paper, the authors established weak interpretations of the Irankuh to all MEMB deposits, without studying other deposits from this belt. The prerequisite of introducing a metallogenic model for a region or a mineralizing belt is to study all geological and geochemical aspects of all deposits and specially check all previous studies accomplished there. The lack of discussion on the data in previous studies (e.g., different deposit types in the MEMB) in this paper undermines the credibility of the proposed model.

Acknowledgments

We thank prof. Stefano Albanese, chief editor of Journal of Geochemical Exploration, and two anonymous reviewers for their very useful and constructive comments. The authors are grateful to S. Rezaei for her help in creating the GIS data base of SH Zn–Pb deposits of Iran.

References

1. Agard, P., Omrani, J., Jolivet, L., Mouthereau, F., 2005. Convergence history across Zagros, Iran: Constraints from collisional and earlier deformation. Int. J. Earth Sci. 94, 401–19.
2. Aghanabati, A., 1998. Major sedimentary and structural units of Iran (map). Scientific Quarterly J. Geosci. 7, 29–30
3. Akbari, Z., 2017. Model for the genesis of Ahangaran Fe-Pb deposit (SE of Malayer), based on ore types, Geochemistry and stable. Shahid Beheshty University unpublished PhD thesis. pp. 311.
4. Allègre, C.J., Manhès, G., Göpel, C., 2008. The major differentiation of the Earth at∼ 4.45 Ga. Earth Planet. Sc. Lett. 267, 386-98.

5. Azizi, H., Jahangiri, A., 2008. Cretaceous subduction-related volcanism in the northern Sanandaj-Sirjan Zone, Iran. J. Geodyn. 45, 178–90.
6. Bagheri, S., Stampfli, G.M., 2008. The Anarak, Jandaq and Posht–e–Badam metamorphic complexes in Central Iran: New geological data, relationships and tectonic implications. Tectonophysics 451,123–55.
7. Boveiri, M., 2016. Ore-bearing Sulphide Facies and Genetic Model of Detrital-Carbonate-Hosted Zn-Pb Mineralization in the Tappehsorkh Deposit, Irankuh Mining district, South Esfahan. Unpublished Ph.D thesis, Tarbiat Modares University, Tehran, Iran, pp. 415.
8. Boveiri, M., Rastad, E., 2018. Nature and origin of dolomitization associated with sulphide mineralization: new insights from the Tappehsorkh Zn-Pb (-Ag-Ba) deposit, Irankuh Mining District, Iran. Geol. J. 53, 1–21.
9. Boveiri, M., Rastad, E., Mohajjel, M., Nakini, A., Haghdoost M., 2015. Structure, texture, mineralogy and genesis of sulphide ore facies in Tappehsorkh detrital-carbonate- hosted Zn-Pb-(Ag) deposit, South of Esfahan. Scientific Quarterly J. Geosci. 25, 221–36.
10. Boveiri, M., Rastad, E., Peter, J.M., 2017. A sub-seafloor hydrothermal syn-sedimentary to early diagenetic origin for the Gushfil Zn-Pb-(Ag-Ba) deposit, south Esfahan, Iran. Neues Jb. Miner. Abh. 194, 61-90.
11. Bradley, D.C., Leach, D.L., 2003. Tectonic controls of Mississippi Valley-type lead–zinc mineralization in orogenic forelands. Miner. Deposita. 38, 652–67.
12. Dickin, A.P., 2018. Radiogenic isotope geology. Cambridge University Press.
13. Ehya, F., Lotfi, M., Rasa, I., 2010. Emarat carbonate-hosted Zn–Pb deposit, Markazi Province, Iran: A geological, mineralogical and isotopic (S, Pb) study. J. Asian Earth Sci. 37, 186–94.
14. Fadaei, M.J., 2018. Geology, Geochemistry and Type of Pb, Zn (Ba-Ag) Mineralization in lower Cretaseous Volcano-Sedimentary Sequences in NW of Golpayegan (Darehnoghreh and Babasheikh Deposits). Msc thesis in Tarbiat Modares University pp. 283.
15. Fadaei, M.J., Rastad, E., Ghaderi, M., 2016. The horizons and ore facies of Lower Cretaceous volcano-sedimentary hosted Darrehnoghreh Pb-Zn deposit in the northwest of Golpaygan, Sanandaj-Sirjan Zone. 8th symposium of Iranian Society of Economic Geology.
16. Ghasemi, A., Talbot, C., 2006. A new tectonic scenario for the Sanandaj–Sirjan Zone (Iran). J. Asian Earth Sci. 26, 683–93.
17. Ghazi, A.M., Pessagno, E.A., Hassanipak, A.A., Kariminia, S.M., Duncan, R.A., Babaie, H.A., 2003. Biostratigraphic zonation and 40Ar–39Ar ages for the Neotethyan Khoy ophiolite of NW Iran. Palaeogeogr. Palaeocl. 193, 311–23.
18. Haghi, A., Niroomand, S., Rajabi, A., Tabbakh Shabani, A.A., 2019. Geology, Isotope Geochemistry and Fluid Inclusion Investigation on the Robat Zn-Pb-Ba Deposit in the Malayer-Esfahan Metallogenic Belt, Iran. Ore Geol. Rev. (Submited).
19. Herzig, P.M., Hannington, M.D., 1995. Polymetallic massive sulfides at the modern seafloor. Ore Geol. Rev. 10, 95-115.
20. Karimpour, M.H., Sadeghi, M., 2018. Dehydration of hot oceanic slab at depth 30–50 km: KEY to formation of Irankuh-Emarat Pb-Zn MVT belt, Central Iran. J. Geochem. Explor. 194, 88–103.

21. Kelley, K., Leach, D., Johnson, C., Clark, J., Fayek, M., Slack, J., 2004a. Textural, compositional, and sulfur isotope variations of sulfide minerals in the Red Dog Zn-Pb-Ag deposits, Brooks Range, Alaska: implications for ore formation. Econ. Geol. 99, 1509–32.
22. Kelley, K.D., Dumoulin, J.A., Jennings, S., 2004b. The Anarraaq Zn-Pb-Ag and barite deposit, northern Alaska: Evidence for replacement of carbonate by barite and sulfides. Econ. Geol. 99, 1577–91.
23. Kelley, K.D., Jennings, S., 2004. A special issue devoted to barite and Zn-Pb-Ag deposits in the Red Dog district, western Brooks Range, northern Alaska. Econ. Geol. 99,1267–80.
24. Leach, D.L., Bradley, D.C., 2010. Huston D, Pisarevsky SA, Taylor RD, Gardoll SJ. Sediment-hosted lead-zinc deposits in Earth history. Econ. Geol. 105, 593–625.
25. Leach, D.L., Sangster, D.F., Kelley, K.D., Large, R.R., Garven, G., Allen, C.R., 2005. Sedimenthosted lead-zinc deposits: A global perspective. Econ. Geol. 2005;100th Anniversary Volume 561–607.
26. Liu, Y., Song, Y., Hou, Z., Yang, Z., Zhang, H., Ma, W., 2015. The Malayer-Esfahan Carbonate-Hosted Pb-Zn Metallogenic Belt in the Zagros Collisional Orogen of Iran: Characteristics and genetic types. Acta Geol. Sin. 89, 1573–94.
27. Liu, Y., Song, Y., Fard, M., Zhou, L., Hou, Z., Kendrick, M.A., 2019. Pyrite Re-Os age constraints on the Irankuh Zn-Pb deposit, Iran, and regional implications. Ore Geol. Rev. 104, 148-159.
28. Lydon, J.W., 1996. Sedimentary exhalative sulphides (SEDEX). Geology of Canadian mineral deposit types Geological Survey of Canada, Geology of Canada 8, 130–52.
29. Mahmoodi, P., 2018. Geochemistry, origin and genesis of sediment-hosted (trrigenous and carbonate) Zn-Pb mineralization in the Haft Savaran, Hossein Abad and Lakan deposits, in southwest and west of Khomeyn. Unpublished Ph.D thesis, Tarbiat Modares University, Tehran, Iran, pp. 350.
30. Mahmoodi, P., Rastad, E., Rajabi, A., Moradpour, M., 2019. Mineralization horizons, stracture and texture, alteration and mineralization stages in the Zn-Pb (Ba) Eastern Haft-Savaran deposit in Malayer-Esfahan metallogenic belt, south of Khomain. Scientific Quarterly J. Geosci. (in press)
31. Mahmoodi, P., Rastad, E., Rajabi, A., Peter, J.M., 2018. Ore facies, mineral chemical and fluid inclusion characteristics of the Hossein-Abad and Western Haft-Savaran sediment-hosted Zn-Pb deposits, Arak Mining District, Iran. Ore Geol. Rev. 95, 342-65.
32. Mahmoudi, S., Corfu, F., Masoudi, F., Mehrabi, B., Mohajjel, M., 2011. U–Pb dating and emplacement history of granitoid plutons in the northern Sanandaj–Sirjan Zone, Iran. J. Asian Earth Sci. 41, 238–49.
33. Mirnejad, H., Simonetti, A., Molasalehi, F., 2011. Pb isotopic compositions of some Zn–Pb deposits and occurrences from Urumieh–Dokhtar and Sanandaj–Sirjan tectonic belts in Iran. Ore Geol. Rev. 39, 181–187.
34. Moghadam, H.S., Stern, R.J., 2011. Geodynamic evolution of Upper Cretaceous Zagros ophiolites: formation of oceanic lithosphere above a nascent subduction zone. Geol. Mag. 148, 762-801.
35. Moghadam, H.S., Stern, R.J., Rahgoshay, M., 2010. The Dehshir ophiolite (central Iran): Geochemical constraints on the origin and evolution of the Inner Zagros ophiolite belt. Geol. Soc. Am. Bull. 122, 1516-7.

36. Moghadam, H.S., Whitechurch, H., Rahgoshay, M., Monsef, I., 2009. Significance of Nain-Baft ophiolitic belt (Iran): Short-lived, transtensional Cretaceous back-arc oceanic basins over the Tethyan subduction zone. C. R. Geosc. 341, 1016–28.
37. Mohajjel, M., Fergusson, C.L., 2014. Jurassic to Cenozoic tectonics of the Zagros Orogen in northwestern Iran. Int. Geol. Rev. 56, 263–87.
38. Mohajjel, M., Fergusson, C.L., Sahandi, M.R., 2003. Cretaceous–Tertiary convergence and continental collision, Sanandaj–Sirjan zone, western Iran. J. Asian Earth Sci. 21, 397–412.
39. Momenzadeh, M., 1976. Stratabound lead–zinc ores in the lower Cretaceous and Jurassic sediments in the Malayer–Esfahan district (west central Iran), lithology, metal content, zonation and genesis [Unpublished Ph.D. thesis]: Heidelberg, University of Heidelberg, 300 p.
40. Mousivand, F., Rastad, E., Meffre, S., Peter, J.M., Solomon, M., Zaw, K., 2011. U–Pb geochronology and Pb isotope characteristics of the Chahgaz volcanogenic massive sulphide deposit, southern Iran. Int. Geol. Rev. 53, 1239–62.
41. Mousivand, F., Rastad, E., Peter, J.M., Maghfouri, S., 2018. Metallogeny of volcanogenic massive sulfide deposits of Iran. Ore Geol. Rev. 95: 974–1007
42. Movahednia, M., Rastad, E., Rajabi, A., González, F., 2018. Evidence for syn-sedimentary faulting and reduced formation environment of the Ab-Bagh SEDEX-type Zn-Pb deposit, South of Shahreza, Sanandaj-Sirjan zone. Scientific Quarterly J. Geosci. 27, 233–44.
43. Nakini, A., 2013, The Structural analysis of Irankuh and Tiran areas (S and W Isfahan). Unpublished M.Sc. thesis, Tehran, Tarbiat Modares University, pp. 182.
44. Peernajmodin, H., 2018. Ore facies, geochemistry and genesis of Zn-Pb-Ba and Fe carbonate-hosted Khan-Abad, KuhKolangeh, Robat and Shams-Abad deposit, South Arak area. Tarbiat Modares University unpublished PhD thesis pp. 340.
45. Peernajmodin, H., Rastad, E., Rajabi, A., 2018. Ore structure and texture, mineralogical and fluid inclusions studies of the KuhKolangeh Zn-Pb-Ba deposit, Malayer- Isfahan metallogenic belt, Southern Arak, Iran. Scientific Quarterly J. Geosci. 27, 287-303.
46. Rajabi, A., 2015, Geological report of the Sahlabad Cr-Cu deposit, Southeast of Sarbisheh, Iran. Unpublished report 10 pp.
47. Rajabi, A., Mahmoodi, P., 2018. The role of framboidal pyrite in determining the genesis of sedimentary ore deposits. 4th symposium of sedimentological society of Iran at: Zanjan, Iran.
48. Rajabi, A., Rastad, E., Canet, C., 2012. Metallogeny of Cretaceous carbonatehosted Zn–Pbdeposits of Iran: geotectonic setting and data integration for future mineral exploration. Int. Geol. Rev. 54, 1649–1672.
49. Rajabi, A., Rastad, E., Canet, C., Alfonso, P., 2015a. The early Cambrian Chahmir shale-hosted Zn–Pb deposit, Central Iran: an example of vent-proximal SEDEX mineralization. Miner. Deposita. 50 (5), 571-590.
50. Rajabi, A., Canet, C., Rastad, E., Alfonso, P., 2015b. Basin evolution and stratigraphic correlation of sedimentary-exhalative Zn–Pb deposits of the Early Cambrian Zarigan–Chahmir Basin, Central Iran. Ore Geol. Rev. 64, 328-353.
51. Rasskazov, S.V., Brandt, S.B., Brandt, I.S., 2010a. Geochronometric Models. Radiogenic Isotopes in Geologic Processes: Springer p. 11–24.

52. Rasskazov, S.V., Brandt, S.B., Brandt, I.S., 2010b. Separated Lead Isotopes. Radiogenic Isotopes in Geologic Processes: Springer p. 231–47.
53. Shahabpour, J., 2005. Tectonic evolution of the orogenic belt in the region located between Kerman and Neyriz. J. Asian Earth Sci. 24, 405–17.
54. Stampfli, G.M., Borel, G., 2002. A plate tectonic model for the Paleozoic and Mesozoic constrained by dynamic plate boundaries and restored synthetic oceanic isochrons. Earth Planet. Sc. Lett. 196, 17–33.
55. Tosdal, R., Wooden, J., Bouse, R., 1999. Pb isotopes, ore deposits, and metallogenic terranes. 1-28.
56. Yarmohammadi, A., 2006. Mineralogy, Geochemistry and Genesis of the Barika gold (and barite and base metal) Mineralization, East of Sardasht, Northwestern Iran. Unpublished M.Sc. thesis. Tarbiat Modares University, Tehran, Iran, pp. 260.
57. Yarmohammadi, A., 2015. Origin and characteristics of ore forming fluids and genetic model of carbonate hosted Zn-Pb deposits in upper part of lower cretaceous sequence, north Tiran basin in NW of Esfahan. Unpublished Ph.D. thesis, Tehran, Tarbiat Modares University, pp. 395.
58. Yarmohammadi, A., Rastad, E., Rajabi, A., 2019. Geochemistry, fluid inclusion study and genesis of the sediment-hosted Zn-Pb (±Ag±Cu) deposits of the Tiran basin, NW of Esfahan, Iran. Neues Jb. Miner. Abh. 193,183–203.

Figure Captions

Fig. 1: **a)** Simplified structural map of Iran (after Aghanabati, 1998; and Rajabi et al., 2015b) and location of major metallogenic belts of the Cretaceous sediment-hosted Zn-Pb (Ag±Cu±Ba) deposits of Iran. ophiolite belts: (1) Sarv-Abad, (2) Kermanshah, (3) Neyriz, (4) Shahr-e-Babak, (5) Dehshir, (6) Nain). **b)** Simplified terrene map of the western Tethysides (modifies after Rajabi et al., 2012, 2015b). Note the location of the Iranian Plate between the Arabian and Eurasia (Turan) plates. **c**) Geodynamic reconstruction model of the Iranian plate (dark grey) from the Early to Late Cretaceous (modified after Rajabi et al. (2012) based on Stampfli and Borel (2002); Bagheri and Stampfli (2008); Ghasemi and Talbot (2005); Moghadam et al. (2009)) and Zn-Pb (Ag±Cu±Ba) mineralizations around the Nain-Baft suture zone. See Rajabi et al. (2012) for more explanation. A, Alborz ranges; CIM, Central Iranian Microcontinent; NB, Nain-Baft extensional back-arc basin; Sb, Sabzevar back-arc basin (indicated by ophiolites); SC, South Caspian basin; SSZ, Sanandaj-Sirjan zone.

Fig 2: Distribution map of the Cretaceous sediment-hosted Zn–Pb (±Ag±Cu±Ba) deposits in the MEMB, SSZ, and the YAMB in the Yazd block. Most of the deposits occur on both sides of the southern portion of the CIGS transitional zone and in the Nain-Baft back-arc super basin that is characterized by ophiolites (Rajabi et al., 2012).
Fig. 3: Generalized schematic columnar section of the Early Cretaceous sequence of the MEMB and western CIGS gradual zone, with the main ore-bearing (sediment-hosted Zn–Pb (±Ag±Cu±Ba)) strata (modified after Momenzadeh (1976) and Rajabi et al. (2012)).

Fig. 4: Generalized lithostratigraphic columnar sections of selected mining districts in the MEMB, SSZ.

Fig. 5: Comparison of tectonic setting models for (**a**) the typical orogenic-related MVT deposits (Leach et al., 2005; 2010) and (**b** and **c**) the Cretaceous-hosted sediment-hosted Zn–Pb (±Ag±Cu±Ba) deposits in the MEMB and YAMB of Iran (c modified after Rajabi et al., 2012). These deposits are concentrated around the Nain-Baft suture zone in the Iranian plate. 1: YAMB; 2: MEMB. CIM: Central Iranian Microcontinent; SSZ: Sanandaj-Sirjan zone; ZTZ: Zagros thrust zone.

Fig. 6: **a** and **b**) Sheeted like stratabound Zn-Pb±Ba mineralization in the uppermost of the Kl unit (silicified and dolomitized limestone, Klsd), best developed concordantly under the marls of the Ks unit, Robat deposit. **c**) Stratiform sideritic Fe-Mn-Pb (±Ba±Cu) mineralization in the Early Cretaceous tuffaceous siltstones and sandstones, Sarchal deposit. **d**) Laminated barite, pyrite, galena and sphalerite (Py + Gn + Sph) in organic matter-bearing limestone, Ravanj deposit. **e**) Laminated framboidal sulphides (light grey), algal-laminated dolomite (dark grey), and sulfide-bearing dolomite (light). Folded dolomitic ore-bearing layers show typical convolute bedding texture. **f**, **g** and **h**) Microscopic photographs (reflected light) of fine-grained laminated (**f** and **h**) and disseminated sulfides in sulfide-rich bands (**g**), hosted in silty limestone, Gushfil deposit. Sp: sphalerite, Py: pyrite, Om: organic matter, Gn: galena.

1

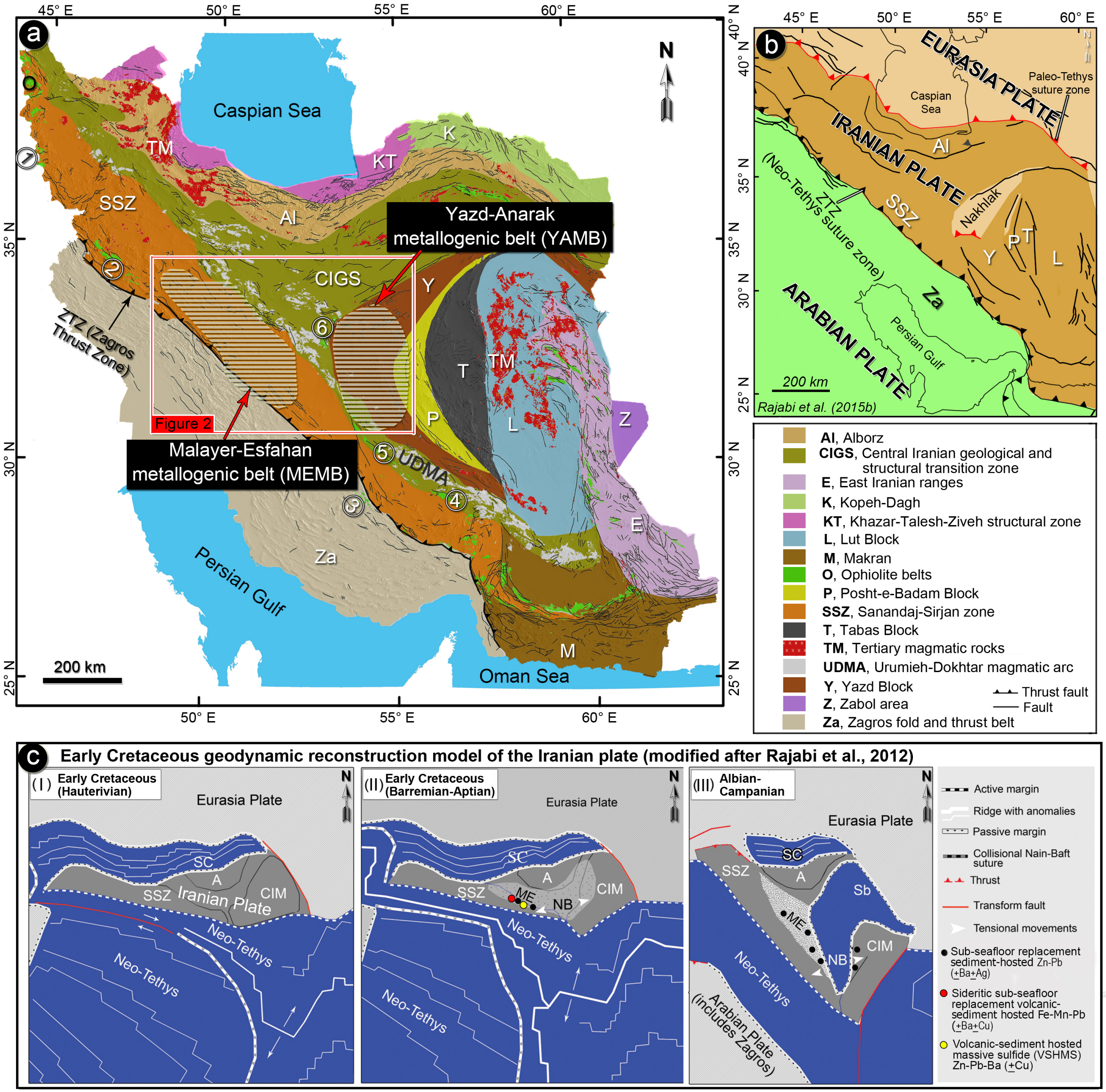

a
Caspian Sea
Persian Gulf
Oman Sea
Yazd-Anarak metallogenic belt (YAMB)
Malayer-Esfahan metallogenic belt (MEMB)
ZTZ (Zagros Thrust Zone)
Figure 2
200 km
45° E
50° E
55° E
60° E
40° N
35° N
30° N
25° N
TM
SSZ
Al
K
KT
CIGS
Y
T
L
P
Z
E
UDMA
Za
M
b
EURASIA PLATE
IRANIAN PLATE
ARABIAN PLATE
Paleo-Tethys suture zone
Caspian Sea
(Neo-Tethys suture zone)
Nakhlak
Persian Gulf
200 km
Rajabi et al. (2015b)
Al, Alborz
CIGS, Central Iranian geological and structural transition zone
E, East Iranian ranges
K, Kopeh-Dagh
KT, Khazar-Talesh-Ziveh structural zone
L, Lut Block
M, Makran
O, Ophiolite belts
P, Posht-e-Badam Block
SSZ, Sanandaj-Sirjan zone
T, Tabas Block
TM, Tertiary magmatic rocks
UDMA, Urumieh-Dokhtar magmatic arc
Y, Yazd Block
Z, Zabol area
Za, Zagros fold and thrust belt
Thrust fault
Fault
c
Early Cretaceous geodynamic reconstruction model of the Iranian plate (modified after Rajabi et al., 2012)
(I) Early Cretaceous (Hauterivian)
(II) Early Cretaceous (Barremian-Aptian)
(III) Albian-Campanian
Eurasia Plate
Iranian Plate
Neo-Tethys
SC
A
SSZ
CIM
ME
NB
Sb
Arabian Plate (includes Zagros)
Active margin
Ridge with anomalies
Passive margin
Collisional Nain-Baft suture
Thrust
Transform fault
Tensional movements
Sub-seafloor replacement sediment-hosted Zn-Pb (±Ba±Ag)
Sideritic sub-seafloor replacement volcanic-sediment hosted Fe-Mn-Pb (±Ba±Cu)
Volcanic-sediment hosted massive sulfide (VSHMS) Zn-Pb-Ba (±Cu)

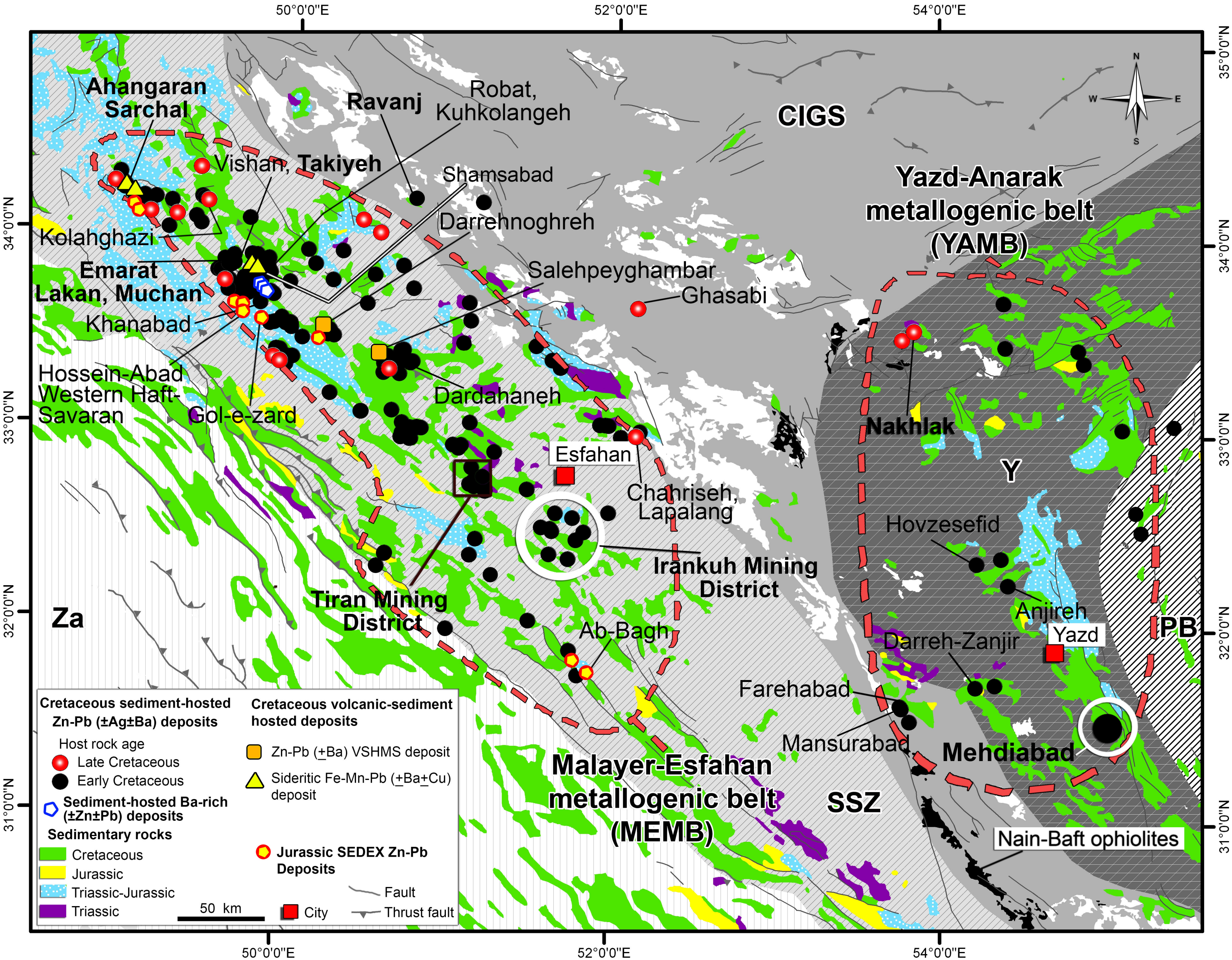

50°0'0"E
52°0'0"E
54°0'0"E
35°0'0"N
34°0'0"N
33°0'0"N
32°0'0"N
31°0'0"N
N
S
W
E
CIGS
Ahangaran
Sarchal
Ravanj
Robat,
Kuhkolangeh
Vishan, Takiyeh
Shamsabad
Darrehnoghreh
Kolahghazi
Emarat
Lakan, Muchan
Salehpeyghambar
Ghasabi
Khanabad
Hossein-Abad
Western Haft-
Savaran
Gol-e-zard
Dardahaneh
Yazd-Anarak
metallogenic belt
(YAMB)
Nakhlak
Y
Esfahan
Chahriseh,
Lapalang
Irankuh Mining
District
Hovzesefid
Tiran Mining
District
Za
Ab-Bagh
Anjireh
PB
Yazd
Darreh-Zanjir
Farehabad
Mansurabad
Mehdiabad
Malayer-Esfahan
metallogenic belt
(MEMB)
SSZ
Nain-Baft ophiolites
Cretaceous sediment-hosted
Zn-Pb (±Ag±Ba) deposits
Host rock age
Late Cretaceous
Early Cretaceous
Sediment-hosted Ba-rich
(±Zn±Pb) deposits
Sedimentary rocks
Cretaceous
Jurassic
Triassic-Jurassic
Triassic
Cretaceous volcanic-sediment
hosted deposits
Zn-Pb (+Ba) VSHMS deposit
Sideritic Fe-Mn-Pb (+Ba+Cu)
deposit
Jurassic SEDEX Zn-Pb
Deposits
Fault
Thrust fault
City
50 km

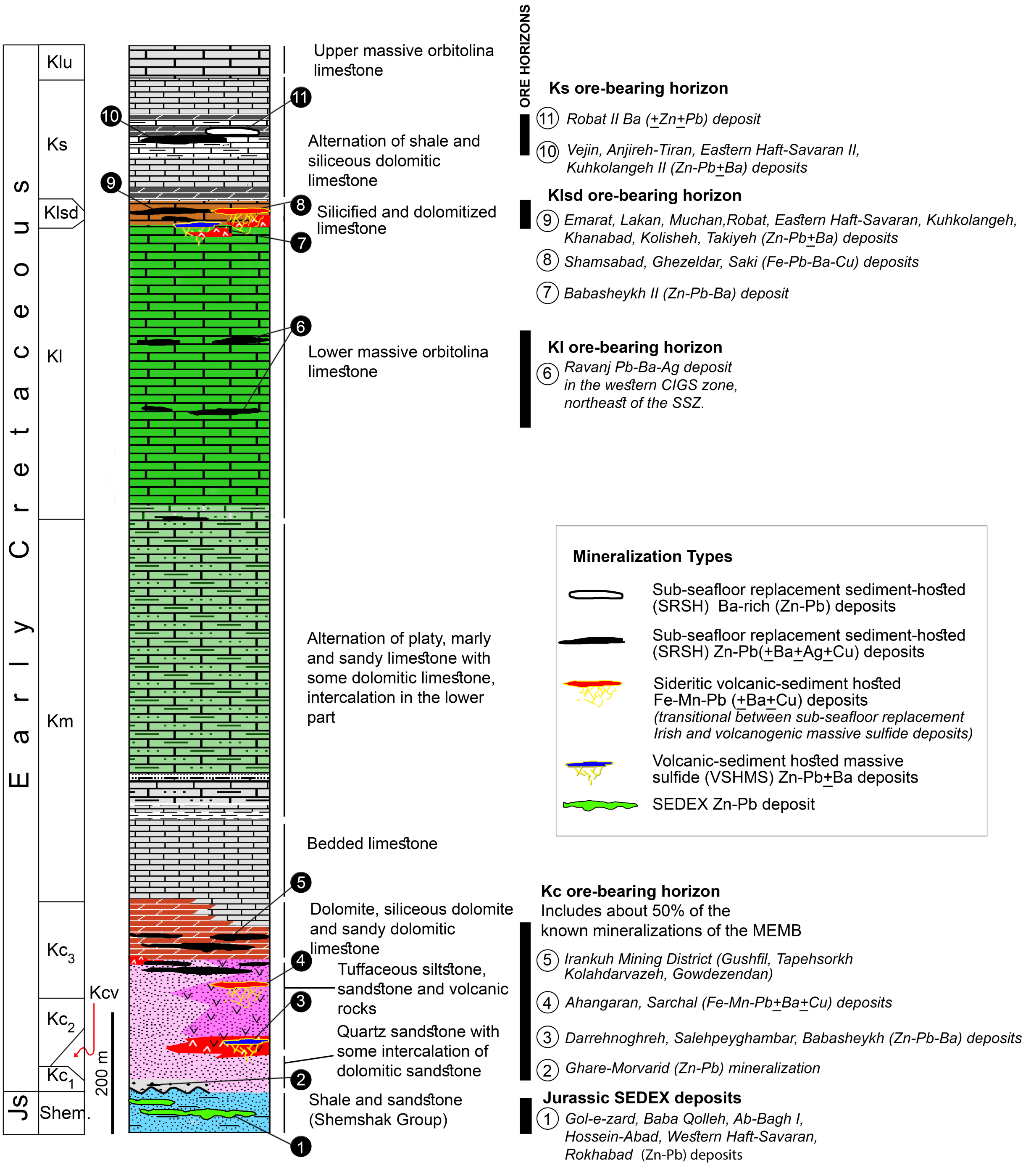

Early Cretaceous
Js
Klu
Ks
Klsd
Kl
Km
Kc3
Kcv
Kc2
Kc1
Shem.
200 m
Upper massive orbitolina limestone
Alternation of shale and siliceous dolomitic limestone
Silicified and dolomitized limestone
Lower massive orbitolina limestone
Alternation of platy, marly and sandy limestone with some dolomitic limestone, intercalation in the lower part
Bedded limestone
Dolomite, siliceous dolomite and sandy dolomitic limestone
Tuffaceous siltstone, sandstone and volcanic rocks
Quartz sandstone with some intercalation of dolomitic sandstone
Shale and sandstone (Shemshak Group)
ORE HORIZONS
Ks ore-bearing horizon
(11) Robat II Ba (+Zn+Pb) deposit
(10) Vejin, Anjireh-Tiran, Eastern Haft-Savaran II, Kuhkolangeh II (Zn-Pb+Ba) deposits
Klsd ore-bearing horizon
(9) Emarat, Lakan, Muchan,Robat, Eastern Haft-Savaran, Kuhkolangeh, Khanabad, Kolisheh, Takiyeh (Zn-Pb+Ba) deposits
(8) Shamsabad, Ghezeldar, Saki (Fe-Pb-Ba-Cu) deposits
(7) Babasheykh II (Zn-Pb-Ba) deposit
Kl ore-bearing horizon
(6) Ravanj Pb-Ba-Ag deposit in the western CIGS zone, northeast of the SSZ.
Mineralization Types
Sub-seafloor replacement sediment-hosted (SRSH) Ba-rich (Zn-Pb) deposits
Sub-seafloor replacement sediment-hosted (SRSH) Zn-Pb(+Ba+Ag+Cu) deposits
Sideritic volcanic-sediment hosted Fe-Mn-Pb (+Ba+Cu) deposits (transitional between sub-seafloor replacement Irish and volcanogenic massive sulfide deposits)
Volcanic-sediment hosted massive sulfide (VSHMS) Zn-Pb+Ba deposits
SEDEX Zn-Pb deposit
Kc ore-bearing horizon
Includes about 50% of the known mineralizations of the MEMB
(5) Irankuh Mining District (Gushfil, Tapehsorkh Kolahdarvazeh, Gowdezendan)
(4) Ahangaran, Sarchal (Fe-Mn-Pb+Ba+Cu) deposits
(3) Darrehnoghreh, Salehpeyghambar, Babasheykh (Zn-Pb-Ba) deposits
(2) Ghare-Morvarid (Zn-Pb) mineralization
Jurassic SEDEX deposits
(1) Gol-e-zard, Baba Qolleh, Ab-Bagh I, Hossein-Abad, Western Haft-Savaran, Rokhabad (Zn-Pb) deposits

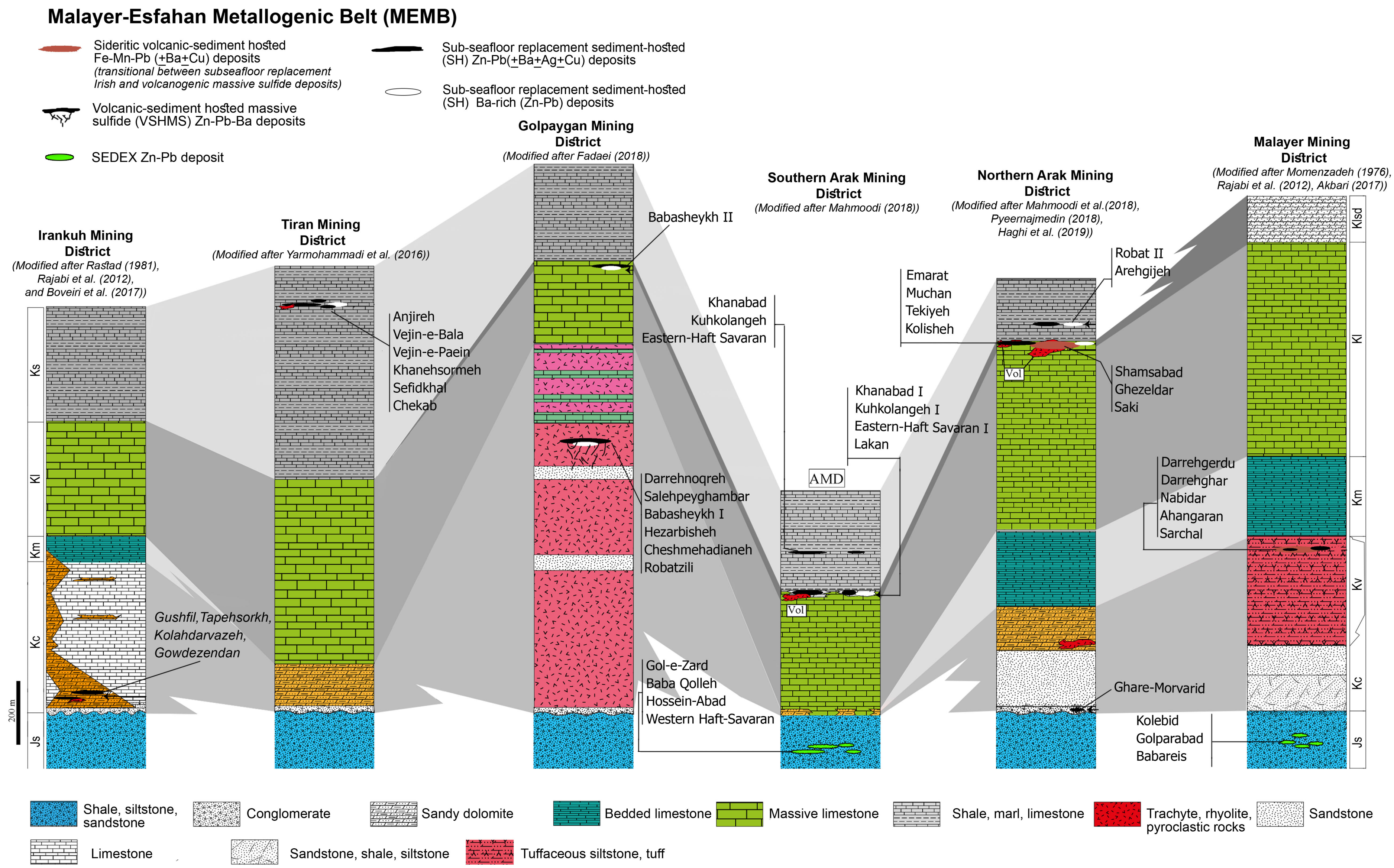

Malayer-Esfahan Metallogenic Belt (MEMB)
Sideritic volcanic-sediment hosted Fe-Mn-Pb (+Ba+Cu) deposits (transitional between subseafloor replacement Irish and volcanogenic massive sulfide deposits)
Sub-seafloor replacement sediment-hosted (SH) Zn-Pb(+Ba+Ag+Cu) deposits
Volcanic-sediment hosted massive sulfide (VSHMS) Zn-Pb-Ba deposits
Sub-seafloor replacement sediment-hosted (SH) Ba-rich (Zn-Pb) deposits
SEDEX Zn-Pb deposit
Irankuh Mining District (Modified after Rastad (1981), Rajabi et al. (2012), and Boveiri et al. (2017))
Tiran Mining District (Modified after Yarmohammadi et al. (2016))
Golpaygan Mining District (Modified after Fadaei (2018))
Southern Arak Mining District (Modified after Mahmoodi (2018))
Northern Arak Mining District (Modified after Mahmoodi et al.(2018), Pyeernajmedin (2018), Haghi et al. (2019))
Malayer Mining District (Modified after Momenzadeh (1976), Rajabi et al. (2012), Akbari (2017))
Ks
Kl
Km
Kc
Js
Kv
Klsd
200 m
Gushfil, Tapehsorkh, Kolahdarvazeh, Gowdezendan
Anjireh
Vejin-e-Bala
Vejin-e-Paein
Khanehsormeh
Sefidkhal
Chekab
Babasheykh II
Darrehnoqreh
Salehpeyghambar
Babasheykh I
Hezarbisheh
Cheshmehadianeh
Robatzili
Gol-e-Zard
Baba Qolleh
Hossein-Abad
Western Haft-Savaran
Khanabad
Kuhkolangeh
Eastern-Haft Savaran
Khanabad I
Kuhkolangeh I
Eastern-Haft Savaran I
Lakan
AMD
Vol
Emarat
Muchan
Tekiyeh
Kolisheh
Robat II
Arehgijeh
Shamsabad
Ghezeldar
Saki
Vol
Darrehgerdu
Darrehghar
Nabidar
Ahangaran
Sarchal
Ghare-Morvarid
Kolebid
Golparabad
Babareis
Shale, siltstone, sandstone
Conglomerate
Sandy dolomite
Bedded limestone
Massive limestone
Shale, marl, limestone
Trachyte, rhyolite, pyroclastic rocks
Sandstone
Limestone
Sandstone, shale, siltstone
Tuffaceous siltstone, tuff

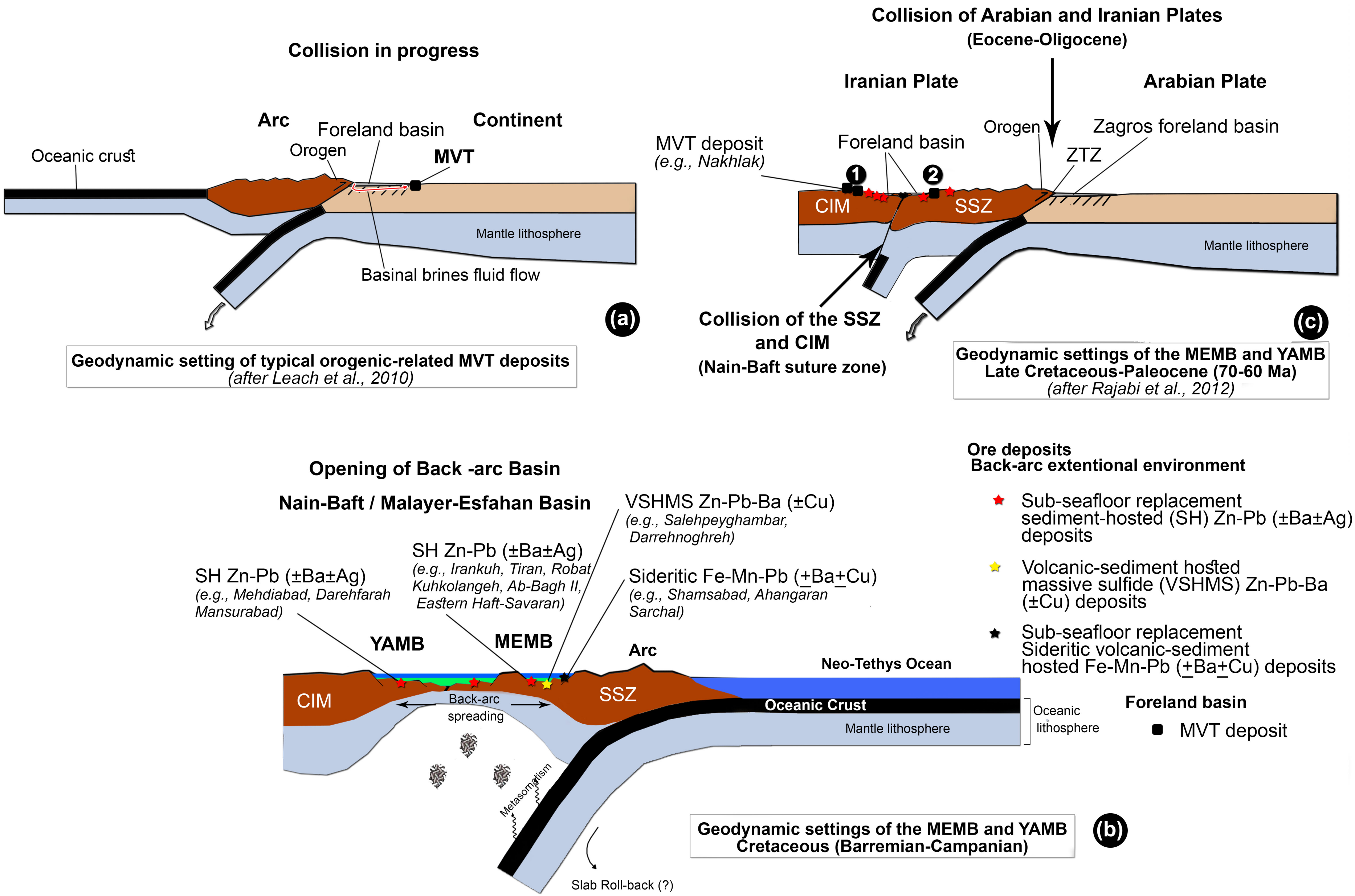
Collision in progress
Arc
Foreland basin
Continent
Oceanic crust
Orogen
MVT
Mantle lithosphere
Basinal brines fluid flow
(a)
Geodynamic setting of typical orogenic-related MVT deposits
(after Leach et al., 2010)
Collision of Arabian and Iranian Plates
(Eocene-Oligocene)
Iranian Plate
Arabian Plate
Orogen
Zagros foreland basin
MVT deposit
(e.g., Nakhlak)
Foreland basin
ZTZ
1
2
CIM
SSZ
Mantle lithosphere
Collision of the SSZ
and CIM
(Nain-Baft suture zone)
(c)
Geodynamic settings of the MEMB and YAMB
Late Cretaceous-Paleocene (70-60 Ma)
(after Rajabi et al., 2012)
Opening of Back -arc Basin
Nain-Baft / Malayer-Esfahan Basin
VSHMS Zn-Pb-Ba (±Cu)
(e.g., Salehpeyghambar,
Darrehnoghreh)
SH Zn-Pb (±Ba±Ag)
(e.g., Irankuh, Tiran, Robat
Kuhkolangeh, Ab-Bagh II,
Eastern Haft-Savaran)
SH Zn-Pb (±Ba±Ag)
(e.g., Mehdiabad, Darehfarah
Mansurabad)
Sideritic Fe-Mn-Pb (+Ba+Cu)
(e.g., Shamsabad, Ahangaran
Sarchal)
YAMB
MEMB
Arc
Neo-Tethys Ocean
CIM
SSZ
Back-arc
spreading
Oceanic Crust
Mantle lithosphere
Oceanic
lithosphere
Metasomatism
Slab Roll-back (?)
Geodynamic settings of the MEMB and YAMB
Cretaceous (Barremian-Campanian)
(b)
Ore deposits
Back-arc extentional environment
Sub-seafloor replacement
sediment-hosted (SH) Zn-Pb (±Ba±Ag)
deposits
Volcanic-sediment hosted
massive sulfide (VSHMS) Zn-Pb-Ba
(±Cu) deposits
Sub-seafloor replacement
Sideritic volcanic-sediment
hosted Fe-Mn-Pb (+Ba+Cu) deposits
Foreland basin
MVT deposit

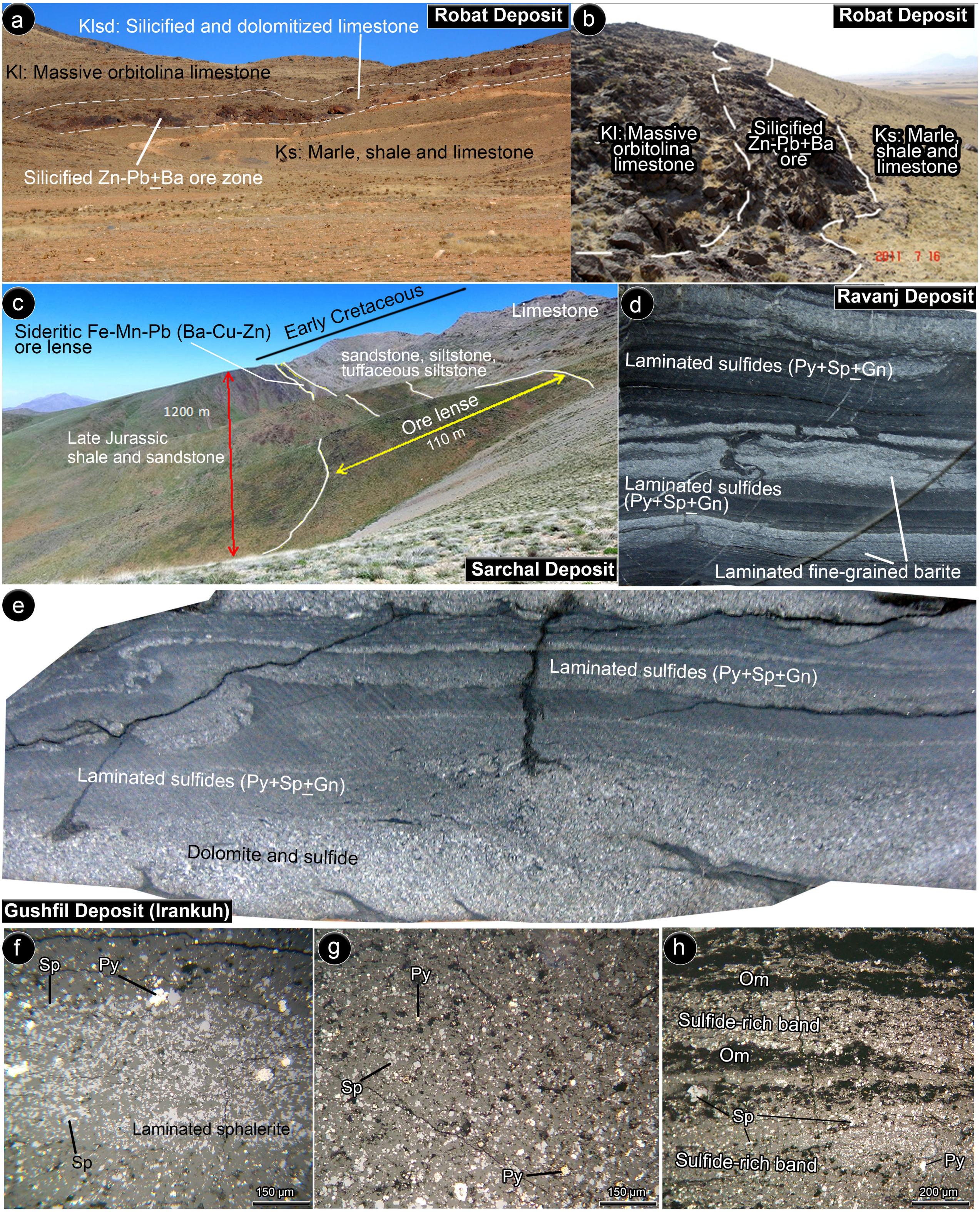
a
Robat Deposit
Klsd: Silicified and dolomitized limestone
Kl: Massive orbitolina limestone
Ks: Marle, shale and limestone
Silicified Zn-Pb±Ba ore zone
b
Robat Deposit
Kl: Massive orbitolina limestone
Silicified Zn-Pb±Ba ore
Ks: Marle, shale and limestone
2011 7 16
c
Sideritic Fe-Mn-Pb (Ba-Cu-Zn) ore lense
Early Cretaceous
Limestone
sandstone, siltstone, tuffaceous siltstone
1200 m
Ore lense
110 m
Late Jurassic shale and sandstone
Sarchal Deposit
d
Ravanj Deposit
Laminated sulfides (Py+Sp±Gn)
Laminated sulfides (Py+Sp±Gn)
Laminated fine-grained barite
e
Laminated sulfides (Py+Sp±Gn)
Laminated sulfides (Py+Sp±Gn)
Dolomite and sulfide
Gushfil Deposit (Irankuh)
f
Sp
Py
Laminated sphalerite
Sp
150 µm
g
Py
Sp
Py
150 µm
h
Om
Sulfide-rich band
Om
Sp
Sulfide-rich band
Py
200 µm